Pergamon

Geochimica et Cosmochimica Acta, Vol. 58, No. 5, pp. 1463–1470, 1994

0016-7037/94 $6.00 + .00

Oxygen isotope composition of garnet and spinel peridotites in the continental mantle: Evidence from the Vitim xenolith suite, southern Siberia

D. A. IONOV,[1,2]* R. S. HARMON,[1†] C. FRANCE-LANORD,[3] P. B. GREENWOOD,[1] and I. V. ASHCHEPKOV[4]

[1]NERC Isotope Geosciences Laboratory, Kingsley Dunham Centre, Keyworth NG12 5GG, UK
[2]Max-Planck-Institut für Chemie (Abteilung Geochemie), Postfach 3060, Mainz 55020, Germany
[3]Centre de Recherches Pétrographiques et Géochemiques, 54501 Vandoeuvre les Nancy, France
[4]United Institute of Geology, Mineralogy and Geophysics, Novosibirsk 630090, Russia

(*Received July* 30, 1992; *accepted in revised form October* 17, 1993)

Abstract—Spinel and garnet facies peridotites from the Vitim Volcanic Field in Siberia comprise a suite of fertile mantle xenoliths, which are LREE depleted and have strongly depleted strontium and neodymium isotopic compositions. Determination of $^{18}O/^{16}O$ ratios by conventional and laser-assisted fluorination techniques yield a very restricted range of whole-rock $\delta^{18}O$ values for both spinel peridotites (+5.4 to +5.8‰) and garnet lherzolites (+5.5 to +5.8‰) equivalent to that observed for lunar rocks and mid-ocean ridge basalts (MORB). Mineral $\delta^{18}O$ values for the xenoliths are: olivine = +5.1 to +5.8‰, orthopyroxene = +5.7 to +6.0‰, clinopyroxene = +5.5 to +6.2‰, garnet = +5.5 to +6.0‰, and spinel = +4.9 to +5.5‰. Similarly, $\delta^{18}O$ ranges for silicate mineral pairs vary from only 0.5 to 0.7‰. The sixteen peridotite xenoliths studied exhibit equilibrium O-isotope fractionations between minerals of a magnitude expected from theoretical and experimental considerations, in particular a temperature-controlled ^{18}O distribution between olivine and pyroxenes in spinel-bearing peridotites.

Because the Vitim garnet and spinel peridotites are rich in basaltic components and show long-term depletion in incompatible elements, they are derived from a MORB-like mantle source which makes up, according to current geochemical models, a predominant part of the Earth's upper mantle. The Vitim xenolith suite may, therefore, reflect its bulk O-isotope character. With increasing temperature and degree of partial melting, such a mantle source could generate basaltic liquids with $\delta^{18}O$ values varying from c.+6.1 to +5.7‰. Thus, the broad $\delta^{18}O$ range of c.+4.5 to +7.5‰ reported in the literature for spinel peridotite xenoliths is probably a very restricted disequilibrium phenomenon that likely reflects recent metasomatic overprinting in highly localized zones of the uppermost continental mantle affected by basaltic magmatism and, therefore, should not be considered as representative of the upper mantle, in general.

INTRODUCTION

THE GREATER PART OF THE Earth's upper mantle is generally considered to consist of peridotite residues remaining after extraction of partial melts from the primitive mantle (e.g., HOFMANN, 1988). The present-day upper mantle includes two major reservoirs: the chemically homogeneous asthenospheric mantle depleted in incompatible elements (MORB-source mantle), and the lithospheric mantle that experienced variable degrees of partial melting and metasomatic enrichment.

Peridotite xenoliths in alkali basalts represent intact fragments of the lithospheric mantle accidently incorporated in ascending basaltic magmas. Previous O-isotope studies (KYSER et al., 1981, 1982; HARMON et al., 1986/7, 1987; KEMPTON et al., 1988; KYSER, 1990; ROSENBAUM et al., 1993) have been restricted almost entirely to the spinel peridotite facies that comprises the thin, uppermost layer (<60 km deep) of the upper mantle. Only very rarely are garnet peridotite xenoliths entrained in alkali basalts, although this is the most abundant lithology in the mantle to depths of at least 400 km (DAWSON, 1980). Garnet peridotite xenoliths are common in kimberlites, but the kimberlite xenoliths probably bear little resemblance to the greater volume of the present-day lithospheric mantle which lies beneath the geologically younger portions of the continents because of the largely refractory and very heterogeneous nature of the Archean mantle through which kimberlite magmas erupt (IONOV et al., 1993).

The large variation in mineral $\delta^{18}O$ values from c.+4.5 to +7.5‰ reported in the literature for spinel peridotite xenolith suites has been attributed to interaction of common, depleted (MORB source-type) mantle with metasomatic fluids derived either from subducted oceanic crust (GREGORY and TAYLOR, 1986a; KEMPTON et al., 1988) or asthenospheric diapirs (ROSENBAUM et al., 1993). However, because oxygen is by far the most abundant element in the mantle (about 50% by weight), the addition of substantial amounts of fluid with distinctly different $\delta^{18}O$ values are required to produce even small shifts in peridotite oxygen isotope composition and, therefore, debate persists whether or not such ^{18}O heterogeneity is a widespread characteristic of the bulk upper mantle (KYSER et al., 1981, 1982) or is instead a very restricted phenomenon arising from localized metasomatic enrichment processes (GREGORY and TAYLOR, 1986a,b; GREGORY and CRISS, 1986).

* *Present address:* School of Earth Sciences, Macquarie University, Sydney, N.S.W., 2109 Australia.
† *Present address:* Geochemisches Institut der Universität, Goldschmidtstrasse 1, 37077 Göttingen, Germany.

We report here new oxygen isotope data for a rare suite of garnet and spinel peridotite xenoliths which are fertile to only moderately depleted in terms of modal and major element composition. Because much of the oxygen isotope data for peridotite xenoliths from alkali basalts in the literature is for samples whose chemical and isotopic composition has been modified by metasomatic alteration (see e.g., GREGORY and TAYLOR, 1986a,b; KEMPTON et al., 1988), the primary aim of this study is to establish the ^{18}O character of the upper mantle source with a depleted, MORB-like trace element composition, which has not been substantially affected either by high-degree partial melting or by metasomatic processes. This can better constrain the ^{18}O character of what appears to be a predominant volume of the present-day upper mantle.

GEOLOGIC SETTING AND SAMPLE DESCRIPTION

The xenoliths studied were collected from a picritic tuff (54°N, 113°E) some 200 km east of Lake Baikal in Siberia. Here, rare xenolith-bearing picritic tuffs (c. 30 Ma), abundant Miocene (18-8 Ma) alkali olivine basalts, and younger (5-2 Ma) basanites and hawaiites comprise the Vitim Volcanic Field, whose origin is associated with asthenospheric uprise and lithospheric rifting in the nearby Baikal rift zone over the last 35-30 Ma (ZONENSHAIN and SAVOSTIN, 1981; ZORIN, 1981).

Some 80% of the mantle xenoliths at the Vitim locality are garnet lherzolites. Less abundant garnet-spinel lithologies, in which aluminous spinel is mantled by garnet in a reaction relationship, are also present. Both garnet and spinel peridotite xenoliths are coarse-grained (typical grain sizes are: ol and opx = 2–5 mm, cpx and spl = 1–2 mm, gar = 5–10 mm), undeformed rocks with protogranular textures. Collectively, the xenoliths encompass a *P-T* range of 850–1200°C and 15–25 kbar (Table 1), corresponding to a depth range of 40–50 km to 75–80 km (IONOV et al., 1993). Thus, the Vitim xenolith suite represents a vertical cross-section through the transitional region of the upper mantle from spinel through garnet-spinel into garnet peridotite facies rocks.

Significantly, the Vitim peridotites comprise one of world's most fertile (i.e., Na-, Ca-, and Al-rich) mantle xenolith suites. The garnet peridotites typically contain abundant clinopyroxene and garnet, which together comprise some 25 ± 5% of the mode (Table 1). In contrast to their fertile mineralogical and major element character, the garnet and spinel peridotites are commonly depleted in light rare earth elements. They also exhibit extremely depleted strontium and neodymium isotopic compositions, which roughly correspond to the DMM-type mantle of ZINDLER and HART (1986) and exhibit concordant Sm-Nd and Rb-Sr model ages (IONOV and JAGOUTZ, 1989). These features suggest that the upper mantle beneath Vitim has experienced an ancient depletion episode at about 2 Ga, in which the degree of melting was low to moderate. Since that time, the Vitim peridotites appear to have been part of a mantle domain that has remained virtually unaffected by large-scale metasomatic enrichment processes (HARMON et al., 1986/7; IONOV et al., 1992). The garnet and spinel peridotite xenoliths exhibit no differences in either major and trace element compositions (IONOV et al., 1993) or in Sr-Nd isotopic character (IONOV and JAGOUTZ, unpubl. data), indicating the general absence of a vertical chemical zonation in the sub-Vitim mantle sampled by the xenoliths.

The Vitim peridotites are distinctly different from those found in kimberlites erupted in the Siberian or South African cratons in terms of modal, major, and trace element composition, and isotopic character. In particular, they are much less depleted in basaltic components and show much less evidence of metasomatic enrichment (IONOV et al., 1993). The Vitim xenolith suite may be characteristic of the continental lithospheric mantle in post-Archean mobile belts (that comprise a much larger part of the present-day continents than the ancient cratons), with relatively little overprint of intra-plate volcanism. It also appears to be chemically similar to the MORB source-type mantle and, therefore, may be representative of the predominant portion of the Earth's upper mantle.

Table 1. Compositional and thermo-barometric data for Vitim peridotite xenoliths (after IONOV et al., 1993)

sample	modal composition (wt. %)					T	P
	ol	opx	cpx	gar	spl	(°C)*	(kbar)*
garnet lherzolites							
313-4	52.2	14.1	14.4	19.3		1122	23.1
313-8	57.0	13.4	15.6	14.0	tr	1143	23.3
313-54	60.6	13.3	14.7	11.4		1149	24.0
313-1	60.8	13.7	12.1	13.4		1084	22.7
313-37	60.6	13.3	14.7	11.4		1149	24.0
313-3	61.1	12.7	14.3	11.9	tr	1105	23.0
313-6	63.7	12.1	12.9	11.3	tr	1147	23.1
313-5	64.0	11.2	13.4	11.4	tr	1193	23.7
garnet spinel lherzolites							
314-230	53.3	30.8	15.2	tr	0.5	1085	19.5
314-580	68.4	15.7	13.5	tr	2.4	1188	23.8
spinel peridotites							
314-56	58.4	19.4	19.2		3.0	945	
314-59	62.0	17	18.8		2.2	1162	
314-58	62.3	18.7	15.7		3.2	980	
86-1	62.8	19.9	14.9		2.3	1102	
314-6	70.4	22.8	5.7		1.1	1046	
314-5	77.7	20.0	1.6		0.7	1108	

*The P-T values calculated after BREY and KÖHLER (1990).

ANALYTICAL METHODS

The standard analytical procedure employed in most laboratories for the determination of oxygen isotope ratios in silicate and oxide rocks and minerals involves the reaction of a sample at a temperature between 200–700°C with either an interhalogen fluoride such as BrF_5 or ClF_3 (BAERTSCHI and SILVERMAN, 1951; CLAYTON and MAYEDA, 1963; BORTHWICK and HARMON, 1982) or with fluorine (CLAYTON and EPSTEIN, 1958; TAYLOR and EPSTEIN, 1962). Typically, 5–30 mg of sample are reacted with the selected reagent in an externally-heated, high-purity nickel reaction vessel for >8 h to liberate oxygen, which is subsequently purified in a stainless steel vacuum system and converted to carbon dioxide by reaction with heated carbon in a glass vacuum system. Hygroscopic NiF_2 is a by-product of the fluorinating agent reacting with the nickel vessel and minor, but significant, contamination, which results from either introduction of water into the reaction vessel by adsorption onto the NiF_2 or the interaction of released oxygen with the NiF_2, is an inevitable result of the technique. Also, the graphite converters used for the O_2-CO_2 step of the process can also produce significant carbon monoxide (TAYLOR and EPSTEIN, 1962), so a platinum catalyst is commonly used to suppress CO production.

Although readily applicable to rock powders and most minerals <200 mesh in grain size, highly refractory and Mg-rich silicate phases like olivine and garnet from peridotite xenoliths are extremely difficult to react using this conventional fluorination technique (see e.g., KYSER et al., 1981; VENNEMANN and SMITH, 1990). This fact may be a factor contributing to the greater spread of olivine $\delta^{18}O$ values relative to those for pyroxene reported for peridotites in the literature (KYSER et al., 1981, 1982; KEMPTON et al., 1988; KYSER, 1990; ROSENBAUM et al., 1993). Therefore, we have utilized a combination of the laser-assisted fluorination technique described recently by SHARP (1990) and the conventional fluorination technique to determine and compare $^{18}O/^{16}O$ ratio measurements for inclusion-free mineral separates (olivine [ol], orthopyroxene [opx], clinopyroxene [cpx], garnet [gar], and spinel [spl]) that had been hand picked from crushed Vitim peridotite xenoliths.

Conventional fluorination analyses were performed at the SMU (Dallas) and NIGL (London and Keyworth) laboratories. Between 5–10 mg of 100% pure bulk mineral separate was ground in acetone or alcohol to <400 mesh in an agate mortar, top-loaded into reaction vessels that were overpressured with dry nitrogen, and reacted at either 600°C (opx, cpx, and spl) or 650–700°C (ol and gar). At SMU, ClF_3 was the reagent used for all mineral analyses whereas, at NIGL, ClF_3 was only used for opx and cpx analyses and BrF_5 was used for ol, gar, and spl analyses. Longer reaction times were utilized

Table 2. Comparison of conventional and laser-assisted fluorination O-isotope data for olivine and garnet from Vitim peridotite xenoliths

Sample	Conventional analyses							Laser-assisted analyses					
	Olivine (NIGL & SMU)			Garnet (NIGL)			Gar (SMU)	Olivine			Garnet		
	#	$\delta^{18}O$ (‰ SMOW)	Yield (%)	#	$\delta^{18}O$ (‰ SMOW)	Yield (%)	$\delta^{18}O$* (‰ SMOW)	#	$\delta^{18}O$ (‰ SMOW)	Yield (%)	#	$\delta^{18}O$ (‰ SMOW)	Yield (%)
313-1	2	5.8±0.3	88	1	6.1	96	7.5				2	5.9±0.5	100
313-3	1	6.1	87	2	7.2±0.7	88	8.1	1	5.5	60	1	5.5	97
313-4	2	5.4±0.0	93	1	6.3	96	6.5				1	5.7	100
313-5	2	5.6±0.3	93	1	7.8	100	7.9	1	5.4	93	1	5.55	96
313-6	1	5.95	92	2	6.25±0.1	96	6	2	5.25±0.0	97	2	5.6±0.0	98
313-8	2	5.5±0.1	93	2	7.0±0.1	98	7.8	2	5.3±0.1	93	2	6.0±0.0	100
313-37	2	5.6±0.4	88	1	6.9	87	7.1	1	5.8	89	1	5.6	97
313-54	4	5.45±0.3	94	1	6.9	96	6.7	2	5.6±0.2	96	2	5.7±0.3	98
314-230	2	5.6±0.3	92										
314-580	2	5.45±0.2	84	1	7.3	100							
314-5	3	5.7±0.1	95										
314-6	1	5.4	94					2	5.4±0.2	-			
314-56	1	5.4	93					1	5.6	97			
314-58	2	5.1±0.0	90					1	5.1	98			
314-59	1	5.7	97					1	5.8	94			
86-1	2	5.6±0.0	94					3	5.4±0.1	93			

For duplicated analyses an average and standard deviation (1σ) are shown. *All yields at SMU are >90%.

for ol and gar (2–3 days) than for opx, cpx, and spl (10–18 h). Oxygen yields for the conventional analyses were 98–102% for opx and cpx as compared with 84–100% for ol, gar, and spl (Table 2). Average precision based upon replicate analysis of twenty-four random samples (Table 2) was better than 0.2‰ (±1σ). Reference sample NBS-28 has a value of +9.66‰ relative to V-SMOW in the SMU laboratory and +9.62‰ in the NIGL laboratory.

A few pyroxenes and the refractory phases ol, gar, and spl were also analyzed at CRPG (Nancy) using the laser ablation fluorination technique. A 20 W CO_2 laser was used to heat 2–10 grains (c. 2–4 mg) of mineral separate in a stainless steel chamber fitted with a BaF_2 window and filled with BrF_5 to a pressure of c. 0.15 atm. Both SHARP (1990) and MATTEY and MACPHERSON (1993) have noted that low $\delta^{18}O$ values can be produced for highly refractory minerals by the laser fluorination technique when fluorination reactions are incomplete. Therefore, each ablation reaction was continued until total consumption of the mineral was achieved, which normally took 3–5 min for pyroxenes and about 10 minutes for the other minerals. The laser was operated with a diffuse beam and at low power density in a controlled pulse duration/energy mode throughout the reaction to prevent excessive heating of grains, which would have resulted in sputter and resultant loss of material from the sample holder during reaction. When the grains began to glow, the power was slowly increased and the beam rastered continuously across the sample; the reaction was considered complete when incandescence was no longer observed in the solid fluoride residue.

Following laser heating and sample reaction, the excess reagent was frozen back into a central reservoir and the liberated O_2 passed through a KBr trap to remove any residual fluorine or halogen oxyfluoride compounds. The purified oxygen was converted to CO_2 by reaction with carbon at ca. 750°C. Two different converters were used during the course of the analytical work at CRPG. The first was an internally-heated design in which graphite rod wrapped with platinum wire was suspended between tungsten electrodes; the second was an externally-heated design utilizing a piece of graphite rod wrapped in platinum wire that was placed in a silica tube. Procedural blanks, produced by heating the empty sample tray, were in the range of 0.05–0.1 μmol. Yields for the laser fluorination runs, with two exceptions, were between 93–100% (Table 2).

MATTEY and MACPHERSON (1993) have drawn attention to the fact that laser fluorination yields are determined not only by the extent to which the sample is totally consumed during the primary laser ablation reaction, but also may be influenced by the secondary oxygen to carbon dioxide conversion step. They note that it is the conversion step of the laser fluorination process that will govern both the size of sample that can be analyzed and overall uncertainty of the $^{18}O/^{16}O$ ratio determination and call attention to an isotope effect associated with the O_2-CO_2 conversion step of their procedure that results in low $\delta^{13}C$ and $\delta^{18}O$ values for small (<ca. 750 μg) samples. Unlike the laser fluorination vacuum line design utilized by SHARP (1990), which employs a Hg-diffusion pump as a post-reaction fluorine getter, the CRPG system utilized in this study is similar to that at RHBNC described by MATTEY and MACPHERSON (1993), in that any residual fluorine remaining in the metal vacuum line after post-reaction freeze-down into the reagent reservoir is removed from the oxygen sample by passage through a warm (120°C) KBr trap.

The possibility of fractionation occurring as a result of incomplete O_2-CO_2 conversion was tested with a CRPG internal O_2 standard (O_2N45c). A small amount effect was observed for the internally-heated furnace, such that samples producing <25 μmol of CO_2 exhibited a slight enrichment in ^{18}O attributable to low yield during conversion. For the externally-heated furnace, no amount effect was observed for sample sizes as small as 4 μmol. Therefore, the internally heated graphite reactor in the CRPG laser-assisted fluorination system was calibrated for variable sample size using a pure O_2 gas standard and the analytical data for the small samples corrected in a manner analogous to that described by MATTEY and MACPHERSON (1993).

We undertook a careful interlaboratory comparison to insure that the results obtained in three laboratories can be directly compared. Five quartz samples spanning a 25‰ range were repeatedly analyzed at the SMU and NIGL laboratories, the analyses yielded $\delta^{18}O$ values within the analytical uncertainty. Comparison between the Nancy and NIGL laboratories was carried out using biotite NBS-30 which easily reacts in both conventional and laser techniques. Thirteen analyses of that reference sample gave a consistent $\delta^{18}O$ value of +4.11 ± 0.18‰ at the Nancy laboratory, compared with the accepted value of +5.10‰ relative to V-SMOW, which was obtained in the Keyworth laboratory by conventional fluorination. In addition, an aliquot of CO_2 gas prepared from the Nancy internal reference oxygen sample was analyzed at both the Nancy laboratory ($\delta^{18}O = -35.5$‰) and the Keyworth laboratory ($\delta^{18}O = -34.6$‰). Based upon these results, the Nancy laser fluorination analyses were adjusted by +0.9‰.

The laser ablation fluorination [laf] analyses for the two pyroxenes analyzed reproduced the $\delta^{18}O$ values obtained by the conventional fluorination [cf] within analytical uncertainty (313-6 opx by cf = +5.9‰ vs. by laf = +6.0‰; cpx by cf = +5.7‰ vs. by laf = +5.7‰). The laf results for ol and spl also compare well with the conventional analyses (within ±0.2‰ except for ol samples 313-3 and 313-6; Table 2), and appear to be somewhat more consistent suggesting that single aberrant conventional analyses may be erroneous. In particular, the single $\delta^{18}O$ value of +6.1‰ for ol 313-3 from conventional fluorination appears to be too high when viewed in the context of the $\delta^{18}O$ data for the other minerals in this sample and the other Vitim ol separates analyzed, therefore, the laser-assisted fluorination $\delta^{18}O$ value for this sample is the result reported in Table 3. For all other instances where ol or spl were analyzed by both techniques, we have pooled the results and calculated averages of the conventional and laser-assisted fluorination data (Table 3), with a

precision of ca. ±0.2–0.3‰. In general, olivine, pyroxene, and spinel analyses obtained by the conventional technique and the laser technique are in excellent agreement and exhibit only small ranges in measured $\delta^{18}O$ values. The main advantage of laser-based techniques over conventional fluorination for these minerals appears to be that one can analyze smaller amounts of material more easily.

For garnet, by contrast, laser-assisted fluorination $\delta^{18}O$ values are 0.2–2‰ lower than those obtained by conventional fluorination (Table 2). The discrepancy is due to the fact that garnet results obtained by the conventional technique in both laboratories (SMU and NIGL), utilizing different reagents and run conditions, are very high and range from 6.1 to 8.1‰. It is particularly striking considering the good reproducibility of some of the conventional analyses and the generally high yields of 89–101% obtained (Table 2). By contrast, using the laser technique, the measured $\delta^{18}O$ values for garnet are consistent and of the magnitude predicted from equilibrium considerations. These facts lead us to suspect that the problem lies with the conventional garnet analyses and is a result of the highly refractory nature of endmember Mg garnets, in that their reaction with fluorinating agents at the highest temperatures possible by the conventional technique is even more sluggish than for Mg olivine. If the problem were a general one with a difficulty in analyzing refractory minerals in the SMU and NIGL laboratories (which in the SMU case could be refuted from previously published peridotite data, e.g., (HARMON et al., 1986/87)) then we would see neither the good agreement for the olivine data obtained by conventional analysis at the SMU and NIGL laboratories nor the good agreement for olivine between the conventional and laser techniques.

The dilemma is that the garnet oxygen yields by conventional analyses are seemingly acceptable, but that only this mineral of the five constituting the garnet peridotite xenoliths gave highly erratic and geologically peculiar results. We consider the laser ablation results for gar to be correct because they are similar to the $\delta^{18}O$ values determined for ol, opx, and cpx by both techniques and because the small range of ^{18}O variation observed is consistent with the very restricted variation in major and trace element chemistry (IONOV et al., 1993) that is characteristic of the Vitim garnet peridotites. Our comparative results from both techniques suggest that highly refractory minerals are much more easily reacted using the laser technique. In particular, conventional fluorination analysis of pyrope garnets should be considered with caution if no checks from laser-assisted fluorination are available.

RESULTS AND DISCUSSION

The $^{18}O/^{16}O$ ratios determined for minerals from eight garnet lherzolites, two garnet-spinel lherzolites, and six spinel peridotites are given as $\delta^{18}O$ values (‰ SMOW) in Table 3 and compared with data for other intraplate alkali basalt localities from the literature in Table 4. Also reported in Table 3 are differences in the $\Delta^{18}O$ values between the different phases stated as Δ values, where $\Delta^{18}O_{x-y} = \delta^{18}O_x - \delta^{18}O_y$ and x and y are a coexisting mineral pair. By comparison to most other mantle peridotite xenolith suites worldwide, the Vitim mantle xenoliths exhibit a very limited oxygen isotope variation. Ranges of mineral $\delta^{18}O$ values for Vitim spinel-bearing peridotites are: ol = +5.1 to +5.7‰, opx = +5.7 to +6.0‰, cpx = +5.6 to +6.2‰, and spl = +4.9 to +5.5‰. By comparison, mineral $\delta^{18}O$ ranges for Vitim garnet lherzolites are: ol = +5.4 to +5.8‰, opx = +5.8 to +5.9‰, cpx = +5.5 to +5.7‰, and gar = +5.5 to +6.0‰. The $\Delta^{18}O$ ranges for silicate mineral pairs are small and of similar magnitude: 0.8‰ for opx-ol, 0.6‰ for cpx-ol, 0.7‰ for opx-cpx, 0.7‰ gar-ol, and 0.5‰ for opx-gar (Table 3, Fig. 1). Calculated whole-rock $\delta^{18}O$ values, which for the sixteen xenoliths analyzed vary from only +5.4 to +5.8‰ (mean = +5.6 ± 0.1‰), are equivalent for spinel, spinel-garnet, and garnet facies peridotites indicating that no pressure-dependent isotope fractionation is manifest over the depth interval in the upper mantle from which the Vitim peridotites were derived.

Fractionation of ^{18}O between Coexisting Minerals

Under equilibrium conditions, the fractionation of ^{18}O between two coexisting minerals should vary as an inverse function of temperature and approach zero at very high temperatures (BIGELEISEN and MAYER, 1947). The oxygen isotope systematics of the Vitim peridotites are consistent with

Table 3. Combined O-isotope data for Vitim spinel, spinel-garnet, and garnet peridotite xenoliths

sample	$\delta^{18}O$ (‰ SMOW)						$\Delta^{18}O_{x-y}$ (‰)				
	ol[c,l]	opx[c]	cpx[c]	gar[l]	spl[c,l]	wr*	cpx-ol	opx-ol	gar-ol	opx-cpx	opx-gar
garnet lherzolites											
313-1	5.8[c]	5.8	5.7	5.9		5.8	-0.1	0	0.1	0.1	-0.1
313-3	5.5[l]	5.8	5.5	5.5		5.5	0	0.3	0	0.3	0.2
313-4	5.4[c]	5.9	5.7	5.7		5.6	0.3	0.5	0.3	0.2	0.2
313-5	5.5	5.9	5.7	5.6		5.6	0.2	0.4	0.1	0.2	0.3
313-6	5.5	5.9	5.7	5.6		5.6	0.2	0.4	0	0.1	-0.2
313-8	5.4	5.8	5.7	6.0		5.6	0.3	0.4	0.6	0.1	0.2
313-37	5.7	5.8	5.7	5.6		5.7	0	0.1	-0.1	0.1	0.2
313-54	5.5	5.9	5.7	5.7		5.6	0.2	0.4	0.2	0.2	0.2
spinel-garnet lherzolites											
314-230	5.6[c]	6.0	5.8			5.7	0.2	0.4		0.2	
314-580	5.4[c]	5.7	6.1		4.9	5.6	0.7	0.3		-0.4	
spinel peridotites											
314-5	5.7[c]	5.8	5.8			5.7	0.1	0.1		0	
314-6	5.4	5.7	5.6		5.1	5.5	0.2	0.3		0.1	
314-56	5.5	5.8	5.7			5.6	0.2	0.3		0.1	
314-58	5.1	5.9	5.8		5.4	5.4	0.7	0.8		0.1	
314-59	5.7	5.9	6.2			5.8	0.5	0.2		-0.3	
86-1	5.5	5.8	5.7		5.4	5.6	0.2	0.3		0.1	

[c] $\delta^{18}O$ determination by conventional fluorination (cf), [l] $\delta^{18}O$ determination by laser-assited fluorination (laf), $\delta^{18}O$ values for olivine and spinel are averages of all cf and laf analyses (see Table 2), except in the cases of those labelled with [c] or [l] (the laf $\delta^{18}O$ value for 313-3 olivine was preferred because the single cf $\delta^{18}O$ value appeared aberrantly high). * whole-rock $\delta^{18}O$ values calculated from mineral O-isotope analyses and sample modal compositions (Table 1).

Table 4. Comparison of O-isotope data for peridotite xenoliths from Vitim and other continental intraplate alkali basalt localities

locality	# samples	$\delta^{18}O$ range (‰ SMOW)	reference*
Western U.S.			
Baja	5	+5.9 to +7.0	1
San Carlos	7	+5.4 to +5.6	1
Dish Hill	2	+5.7 to +6.5	1
Kilbourne Hole	3	+5.2 to +5.5	1
Western Europe			
Massif Central	12	+5.3 to +6.8	1,5
Eifel	13	+5.3 to +6.3	3
N. Hessia	23	+5.1 to +7.0	2
Central Asia			
Tariat	11	+4.9 to +5.7	4
Vitim - spl peridotites	6	+5.4 to +5.8	6
- spl-gar peridotites	2	+5.6 to +5.7	6
- gar peridotites	8	+5.5 to +5.8	6

* 1. KYSER et al., 1981; 2. HARMON et al., 1986/87; 3. HARMON et al., 1987; 4. KEMPTON et al., 1988; 5. DOWNES et al., 1991; 6. this study

theoretical predictions (KIEFFER, 1982; CLAYTON and KIEFFER, 1991) and recent experimental observations (CHIBA et al., 1989; ROSENBAUM et al., 1993). Opx is only very slightly enriched in ^{18}O relative to cpx and exhibits somewhat greater ^{18}O enrichment over spl and ol. Ol in garnet peridotites has a similar $^{18}O/^{16}O$ ratio to gar (Table 3).

In Fig. 2, the $\delta^{18}O$ values from Table 3 for ol, cpx, gar, and sp are plotted vs. those for opx. On these $\delta_x - \delta_y$ diagrams, which clearly discriminate between temperature-controlled closed-system equilibrium fractionation and open-system disequilibrium (GREGORY and TAYLOR, 1986a,b; GREGORY and CRISS, 1986), the Vitim data form compact clusters, which lie either parallel to the zero-fractionation line $\Delta^{18}O_{x-y} = 0$ (e.g., cpx-opx and gar-opx) or between the $\Delta^{18}O_{x-y} = 0$ and $\Delta^{18}O_{x-y} = +1$ isotherms (e.g., ol-opx and spl-opx). This situation is in striking contrast with most of the results for peridotite xenoliths worldwide (the shaded fields in Fig. 1) published to date (KYSER et al., 1981, 1982; KEMPTON et al., 1988; KYSER, 1990; ROSENBAUM et al., 1993), which typically exhibit extended, subvertical arrays that crosscut the isotherms on such $\delta_x - \delta_y$ diagrams (in particular, those including ol and sp) with a steep positive slope, and are characteristic of oxygen isotope disequilibrium resulting from an open-system process (GREGORY and TAYLOR, 1986a; GREGORY and CRISS, 1986). This distinct difference further demonstrates the equilibrium nature of the oxygen isotope distribution within the Vitim peridotite xenoliths. Only the spinel peridotites from Tariat, Mongolia studied by HARMON et al. (1986/7), another suite of mantle xenoliths from the Baikal rift zone, which closely resemble the Vitim samples in terms of their chemical and radiogenic isotope compositions, exhibit similar oxygen isotope characteristics.

Observed ^{18}O fractionations between opx and ol ($\Delta^{18}O_{opx\text{-}ol}$) are displayed in Fig. 2 as a function of xenolith petrologic equilibration temperatures (Table 1) calculated on the basis of the recent experimental calibration of BREY and KÖHLER (1990). With the exception of sample 313-37, all of the Vitim peridotites plot within analytical uncertainty of the experimental fractionation curves. For spinel peridotites (the filled symbols in Fig. 2), which equilibrated over a temperature range of ca. 270°C, there is the suggestion of a negative covariation between the petrologic equilibration temperatures and $\Delta^{18}O_{opx\text{-}ol}$ values. This situation is expected from theoretical considerations for equilibrium mineral assemblages (KIEFFER, 1982; CLAYTON and KIEFFER, 1991), but has not previously been observed for individual mantle peridotite suites. The temperature gradient of the ^{18}O fractionations for the Vitim peridotites is somewhat less steep than expected from the experimental calibrations of CHIBA et al. (1989) and ROSENBAUM et al. (1993), but this feature may be either an artifact of the relatively large analytical uncertainties in $\Delta^{18}O_{opx\text{-}ol}$ values (particularly in the case of the low-temperature sample 314-58) or a reflection of the substantial differences in bulk chemical composition between the peridotite minerals and the materials used in the high-temperature, solid-solid exchange experiments.

Petrogenetic Implications

The oxygen isotope composition of a primary basaltic magma will be determined by a variety of factors which include (1) the $^{18}O/^{16}O$ ratio of its mantle protolith, (2) the nature and degree of partial melting, (3) the temperature at which partial melting occurs, and (4) the extent of isotopic exchange and equilibration prior to melt extraction. The $\delta^{18}O$ value of a basaltic melt will more closely reflect that of its mantle source at higher temperatures of fusion, greater degrees of partial melting, the more closely the melting process approaches a Rayleigh process, and the more rapidly melt extraction occurs.

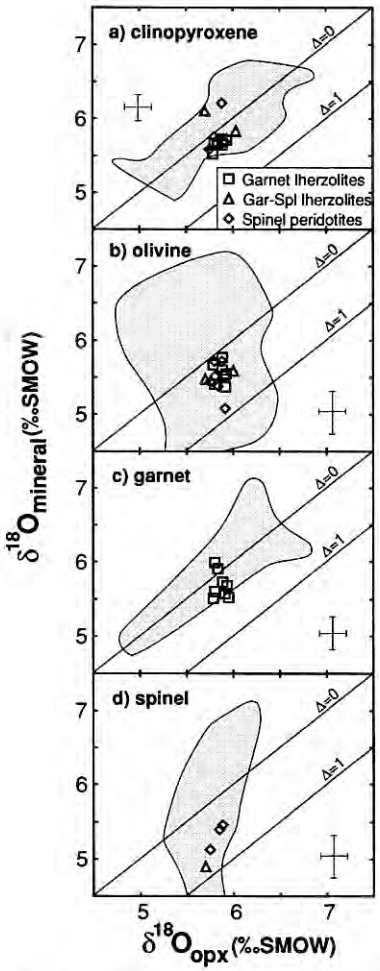

FIG. 1. Plot of $\delta^{18}O$ values of clinopyroxene (a), olivine (b), garnet (c), and spinel (d) vs. orthopyroxene for the Vitim peridotite xenoliths with the symbols as in Fig. 2. Typical $\pm 1\sigma$ uncertainties in $^{18}O/^{16}O$ ratio determinations are indicated by the error bar in each diagram. The shaded areas indicate the fields of $\delta^{18}O$ variation for spinel and garnet peridotite xenoliths from alkali basalt and kimberlite lavas worldwide (KYSER et al., 1981, 1982; HARMON et al., 1986/7, KEMPTON et al., 1988; KYSER, 1990; ROSENBAUM et al., 1993). Note that the Vitim xenoliths exhibit a very restricted range of mineral $\delta^{18}O$ variations and lie between the $\Delta^{18}O = 0$ and $\Delta^{18}O = +1$ isotherms within analytical uncertainty. This contrasts sharply with the worldwide data fields (particularly for olivine-orthopyroxene and spinel-orthopyroxene), which for most localities except Tariat (HARMON et al., 1986/7) and Hawaii (KYSER et al., 1981), exhibit a large range of $\delta^{18}O$ variation and extend well above the $\Delta^{18}O = 0$ line of zero fractionation, features that are indicative of open-system disequilibrium in the upper mantle protolith from which the xenoliths were derived.

The narrow range of whole-rock $\delta^{18}O$ values for the Vitim peridotites is comparable to that observed for lunar rocks (CLAYTON et al., 1971, 1972, 1973) and MORB (MUEHLENBACHS and CLAYTON, 1972; ITO et al., 1987). MORB, the most abundant basalt type on Earth, are generated by large degrees of partial melting of anhydrous, incompatible element depleted mantle peridotite at about 1400°C (BVSP, 1981) and have a very uniform oxygen isotope composition with $\delta^{18}O = +5.7 \pm 0.2‰$. Together, the limited amount of experimental data available (MUEHLENBACHS and KUSHIRO, 1974) and empirical observations on $^{18}O/^{16}O$ ratios in phenocrysts and groundmass of basaltic lavas (GARLICK, 1966; ANDERSON et al., 1971; KYSER et al., 1981; SHEPPARD and HARRIS, 1985) suggests that melt-mineral ^{18}O fractionations are extremely small at the high temperatures at which mantle melting occurs, with derivative basaltic melts only very slightly enriched in ^{18}O relative to the residual mineralogy (ol, opx, ±cpx, ±cr-spl) of the source protolith. Therefore, a genetic relationship may exist between the sub-Vitim mantle and the MORB-source, which is also consistent with the LREE depletion and radiogenic isotope systematics of the Vitim peridotite xenoliths (IONOV and JAGOUTZ, 1989; IONOV et al., 1993).

Oceanic intraplate basalts (OIB), which are more diverse in petrological and geochemical character than MORB, also are much more variable in ^{18}O content, with tholeiites generally having lower $\delta^{18}O$ values than alkalic lavas (HARMON and HOEFS, 1993). Current petrogenetic models for OIB typically envisage small degrees of partial melting of diapirically-uprising plumes, derived from heterogeneous reservoirs within the deep mantle, that may also interact with the depleted asthenospheric mantle and oceanic lithosphere during ascent. The ca. 2‰ range of $\delta^{18}O$ values for OIB is consistent with a petrogenesis dominated by small amounts of partial melting of isotopically distinct sources.

However, the results of this study suggest that a portion of the ^{18}O variation observed in OIB may reflect differences in the temperature at which partial melting or final melt-residue equilibration occurs. Because melt-mineral ^{18}O fractionation may be a few tenths permil more pronounced at ca. 1100–1200°C than at c. 1400°C (Fig. 2), partial melting of the same mantle source at different temperature could produce lavas with slightly different $\delta^{18}O$ values, presuming that the liquid behaves as an ideal mixture of phase components whose fractionation factors follow closely the solid-

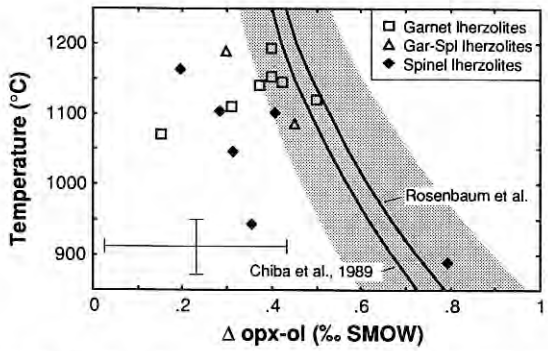

FIG. 2. Plot of $\Delta^{18}O_{opx\text{-}ol}$ (i.e., $\delta^{18}O$ value for orthopyroxene minus $\delta^{18}O$ value for olivine) vs. petrologic equilibration temperature calculated by IONOV et al. (1993) from the technique of BREY and KÖHLER (1990) for Vitim peridotite xenoliths. Garnet lherzolites are indicated by open squares, garnet-spinel lherzolites by open triangles, and spinel lherzolites by filled diamonds. Also shown on the diagram are experimentally determined relationships for the temperature dependence of the diopside-forsterite ^{18}O fractionation from CHIBA et al. (1989) and ROSENBAUM et al. (1993). The shaded area denotes the uncertainty interval for the ROSENBAUM et al. (1993) curve and the error bar indicates the cumulative uncertainty in the calculated temperature and $\Delta^{18}O_{opx\text{-}ol}$ values. See text for discussion.

solid fractionations at the temperature of the liquid. For example, partial melting of the average Vitim peridotite at 1200°C would produce a basaltic liquid with a $\delta^{18}O$ value of +6.1‰, if the respective olivine-melt and pyroxene-melt fractionations are in the vicinity of −0.5 and +0.2‰, as estimated at present (KYSER, 1990). By contrast, partial melting of the same source at 1400°C would have a $\delta^{18}O$ value of +5.7‰, close to that of MORB, because of the smaller melt-mineral oxygen isotope differences and higher melt-residue ratio. Thus, a heterogeneous mantle source need not be invoked to explain basalt ^{18}O differences of less than 0.5‰.

Whole-rock $\delta^{18}O$ values for the Vitim xenoliths (Table 3) are identical for the spinel and garnet peridotites, demonstrating that no differences in oxygen isotope composition exist between the spinel and garnet peridotite facies in this region of the continental mantle. The whole-rock $^{18}O/^{16}O$ ratios for the Vitim peridotites fall into a very restricted interval of $\delta^{18}O$ = +5.4 to +5.8‰ (avg. = +5.6 ± 0.1‰), which may be characteristic of normal continental mantle not modified by metasomatic processes. This conclusion adds support to the ideas of GREGORY and TAYLOR (1986a), GREGORY and CRISS (1986), and KEMPTON et al. (1988) that the ^{18}O-enriched character of some mantle peridotite xenoliths, which is usually attributed to some form of alteration process within the upper mantle, cannot be a mantle-wide phenomenon.

Oxygen isotope compositions of garnets from mantle peridotites have been reported for very few samples from South African kimberlites (KYSER et al., 1982), with $\delta^{18}O$ values ranging from +4.9 to +7.1‰. Our data for the Vitim xenoliths define a much more restricted $\delta^{18}O$ range of +5.5 to +6.0‰, and suggest the following order of ^{18}O enrichment for the minerals of garnet-bearing lherzolites: opx ≥ cpx > gar = ol. The $\delta^{18}O$ values for other minerals in peridotite xenoliths from kimberlites also exhibit a broad range of ^{18}O variation, which may be a reflection of the extremely fractionated and heterogeneous nature of the lithospheric mantle beneath the Archean cratons through which kimberlite magmas erupt.

By contrast, the sub-Vitim mantle is relatively homogeneous and displays equilibrium oxygen isotope distributions between minerals. Therefore, it may be representative, in a broad sense, of the larger part of the present-day continental lithospheric mantle outside Archean cratons, if metasomatic alteration of small domains of this mantle is largely restricted to localized areas of intensive intraplate basaltic volcanism and the continental-margin regions affected by subduction. This conclusion is supported by the fact that spinel peridotite xenoliths from the Tariat locality in Mongolia, studied by HARMON et al. (1986/7), have similar oxygen isotope characteristics to those observed at Vitim. One can also speculate that the oxygen isotope composition of the Vitim garnet and spinel peridotites also reflects, in general, that of the MORB-like asthenospheric upper mantle as suggested by apparent similarity of their mineralogy, major and trace element composition, and radiogenic isotope signatures. The narrow range of oxygen isotope variation in MORB requires a mantle source region that must be very homogeneous in terms of its bulk composition and oxygen isotope character on a global scale, and the Vitim peridotites may be the first direct evidence for such a source.

Acknowledgments—Thanks are due to the late J. Borthwick of SMU and to H. Sloane of NIGL for laboratory assistance as well as to P. D. Kempton of NIGL and H.-G. Stosch of the University of Cologne for thoughtful discussions on the general topic of mantle O-isotope geochemistry. This work, which constitutes NIGL Publication Series Report #31 and CRPG Contribution #974, was supported, in part, by NSF grant EAR87-08494 to RSH and an Alexander von Humboldt Research Fellowship to DAI. The manuscript benefited considerably from reviews by J. Hoefs, R. T. Gregory, and two anonymous reviewers.

Editorial handling: G. Faure

REFERENCES

ANDERSON A. T., CLAYTON R. N., and MAYEDA T. K. (1971) Oxygen isotope thermometry of mafic igneous rocks. *J. Geol.* **79,** 715–729.

BAERTSCHI P. and SILVERMAN S. R. (1951) The determination of relative abundances of the oxygen isotopes in silicate rocks. *Geochim. Cosmochim. Acta* **1,** 317–328.

Basaltic Volcanism Study Project (1981) *Basaltic Volcanism on the Terrestrial Planets.* Pergamon Press.

BIGELEISEN J. and MAYER M. G. (1947) Calculation of equilibrium constants for isotope exchange reactions. *J. Chem. Phys.* **15,** 261–267.

BORTHWICK J. and HARMON R. S. (1982) A note regarding ClF_3 as an alternative to BrF_5 for oxygen isotopic analysis. *Geochim. Cosmochim. Acta* **46,** 1665–1668.

BREY G. P. and KÖHLER T. (1990) Geothermobarometry in four-phase lherzolites II. New thermobarometers and practical assessment of existing thermobarometers. *J. Petrol.* **31,** 1353–1378.

CHIBA H., CHACKO T., CLAYTON R. N., and GOLDSMITH J. R. (1989) Oxygen isotope fractionations involving diopside, forsterite, magnetite, and calcite: Application to geothermometry. *Geochim. Cosmochim. Acta* **53,** 2985–2995.

CLAYTON R. N. and MAYEDA T. K. (1963) The use of bromine pentafluoride in the extraction of oxygen from oxides and silicates for isotopic analysis. *Geochim. Cosmochim. Acta* **53,** 43–52.

CLAYTON R. N. and KIEFFER S. W. (1991) Oxygen isotopic thermometer calibrations. In *Stable Isotope Geochemistry: A Tribute to Samuel Epstein* (ed. H. P. Taylor, J. R. O'Neil, and I. R. Kaplan); *Geochem. Soc. Spec. Pub.* **3,** 3–10.

CLAYTON R. N., ONUMA N., and MAYEDA T. K. (1971) Oxygen isotope fractionation in Apollo 12 rocks and soils. *Proc. 2nd Lunar Sci. Conf., Geochim. Cosmochim. Acta Suppl.* **2,** 1417–1420.

CLAYTON R. N., HURD J. M., and MAYEDA T. K. (1972) Oxygen isotopic compositions and oxygen concentrations of Apollo 14 and Apollo 15 rocks and soils. *Proc. 3rd Lunar Sci. Conf., Geochim. Cosmochim. Acta Suppl.* **3,** 1455–1463.

CLAYTON R. N., HURD J. M., and MAYEDA T. K. (1973) Oxygen compositions of Apollo 15, 16 and 17 samples, and their bearing on lunar origin and petrogenesis. *Proc. 4th Lunar Sci. Conf., Geochim. Cosmochim. Acta Suppl.* **4,** 1535–1542.

DAWSON J. B. (1980) *Kimberlites and Their Xenoliths.* Springer-Verlag.

DOWNES H., BRIOT D., KEMPTON P. D., HARMON R. S., and LEYREROUP A. F. (1991) Lower crustal compositions and processes: Pb and O isotope evidence from granulite facies xenoliths, French Massif Central. *Earth Planet. Sci. Lett.* **102,** 342–357.

GARLICK G. D. (1966) Oxygen isotope fractionation in igneous rocks. *Earth Planet. Sci. Lett.* **1,** 361–368.

GREGORY R. T. and CRISS R. E. (1986) Isotopic exchange in open and closed systems. In *Stable Isotopes in High Temperature Geological Processes* (ed. J. W. VALLEY et al.); *Rev. Mineral.* **16,** 91–126. Mineral. Soc. Amer.

GREGORY R. T. and TAYLOR H. P. (1986a) Non-equilibrium metasomatic $^{18}O/^{16}O$ effects in upper mantle mineral assemblages. *Contrib. Mineral. Petrol.* **93,** 124–135.

GREGORY R. T. and TAYLOR (1986b) Possible non-equilibrium oxygen isotope effects in mantle modules, an alternative to the Kyser-O'Neil-Carmichael $^{18}O/^{16}O$ geothermometer. *Contrib. Mineral. Petrol.* **93,** 114–119.

HARMON R. S. and HOEFS J. (1993) Oxygen isotope heterogeneity of the mantle deduced from a global analysis of basalts from different geotectonic settings. *Contrib. Mineral. Petrol.* (submitted).

HARMON R. S., HOEFS J., and WEDEPOHL K.-H. (1987) Stable isotope (O, S, H) relationships in Tertiary basalts and their mantle xenoliths from the Northern Hessian Depression, W. Germany. *Contrib. Mineral. Petrol.* **95,** 350–369.

HARMON R. S., KEMPTON P. D., STOSCH H-G, HOEFS J., and IONOV D. A. (1986/7) $^{18}O/^{16}O$ ratios in anhydrous spinel lherzolite xenoliths from the Shavaryn-Tsaram volcano, Mongolia. *Earth Planet. Sci. Lett.* **81,** 193–202.

HOFMANN A. W. (1988) Chemical differentiation of the Earth: the relationship between mantle, continental crust, and oceanic crust. *Earth Planet. Sci. Lett.* **90,** 297–314.

IONOV D. A. and JAGOUTZ E. (1989) Sr and Nd isotopic composition in minerals of garnet and spinel peridotite xenoliths from the Vitim Highland: First data for mantle inclusions in the USSR. *Trans. (Doklady) USSR Acad. Sci.: Earth Sci. Sect.* **301,** 232–236.

IONOV D. A., KRAMM U., and STOSCH H.-G. (1992) Evolution of the upper mantle beneath the southern Baikal rift zone: An Sr-Nd isotope study of xenoliths from the Bartoy volcanoes. *Contrib. Mineral. Petrol.* **111,** 235–247.

IONOV D. A., ASHCHEPKOV I. V., STOSCH H.-G., WITT-EICKSCHEN G., and SECK H. A. (1993) Garnet peridotite xenoliths from the Vitim volcanic field, Baikal region: The nature of the garnet-spinel peridotite transition zone in the continental mantle. *J. Petrol.* **34,** 1141–1175.

ITO E., WHITE W. M., and GOPEL C. (1987) The O, Sr, Nd, and Pb isotope geochemistry of MORB. *Chem. Geol.* **62,** 157–176.

KEMPTON P. D., HARMON R. S., STOSCH H.-G., HOEFS J., and HAWKESWORTH C. J. (1988) Open-system O-isotope behavior and trace element enrichment in the sub-Eifel mantle. *Earth Planet. Sci. Lett.* **89,** 273–287.

KIEFFER S. W. (1982) Thermodynamics and lattice vibrations of minerals: 5. Applications to phase equilibria, isotopic fractionation, and high-temperature thermodynamic properties. *Rev. Geophys. Space Phys.* **20,** 827–849.

KYSER T. K. (1990) Stable isotopes in the continental lithospheric mantle. In *Continental Mantle* (ed. M. Menzies), pp. 127–156. Clarendon Press.

KYSER T. K., O'NEIL J. R., and CARMICHAEL I. S. E. (1981) Oxygen isotope thermometry of basic lavas and mantle nodules. *Contrib. Mineral. Petrol.* **77,** 11–23.

KYSER T. K., O'NEIL J. R., and CARMICHAEL I. S. E. (1982) Genetic relations among basic lavas and ultramafic nodules: Evidence from oxygen isotope compositions. *Contrib. Mineral. Petrol.* **81,** 88–102.

MATTEY D. and MACPHERSON C. (1993) High-precision oxygen isotope micro-analysis of ferromagnesian minerals by laser-fluorination. *Chem. Geol. (Isotope Geosci. Sect.)* **105,** 305–318.

MUEHLENBACHS K. and CLAYTON R. N. (1972) Oxygen isotope studies of fresh and weathered submarine basalts. *Canadian J. Earth Sci.* **9,** 172–184.

MUEHLENBACHS K. and KUSHIRO I. (1974) Oxygen isotope exchange and equilibria of silicates with CO_2 or O_2. *Carnegie Inst. Wash. Yearb.* **73,** 232–236.

ROSENBAUM J. M., KYSER T. K., and WALKER D. (1993) High temperature oxygen isotope fractionation in the enstatite-olivine-$BaCO_3$ system. *Geochim. Cosmochim. Acta* (submitted).

SHARP Z. D. (1990) A laser-based microanalytical method for the in situ determination of oxygen isotope ratios of silicates and oxides. *Geochim. Cosmochim. Acta* **54,** 1353–1357.

SHEPPARD S. M. F. and HARRIS C. (1985) Hydrogen and oxygen isotope geochemistry of Ascension Island lavas and granites: variations with crystal fractionation and interaction with seawater. *Contrib. Mineral. Petrol.* **91,** 74–81.

TAYLOR H. P. and EPSTEIN S. (1962) The relationship between $^{18}O/^{16}O$ ratios of coexisting minerals of igneous and metamorphic rocks. *Bull. Geol. Soc. Amer.* **73,** 461–480.

VENNEMANN T. W. and SMITH H. S. (1990) The rate and temperature of reaction of ClF_3 with silicate minerals, and their relevance to oxygen isotope analysis. *Chem. Geol. (Isotope Geol. Sect.)* **83,** 83–88.

ZINDLER A. and HART S. (1986) Chemical geodynamics. *Ann. Rev. Earth Planet. Sci.* **14,** 493–571.

ZONENSHAIN L. P. and SAVOSTIN L. A. (1981) Geodynamics of the Baikal rift zone and plate tectonics of Asia. *Tectonophysics* **76,** 1–45.

ZORIN Y. A. (1981) The Baikal rift: An example of the intrusion of asthenospheric mantle into the lithosphere as the cause of the disruption of lithospheric plates. *Tectonophysics* **73,** 91–104.